2321-8045 Science Park Research Journal Vol-2, Issue- 35, 12th March 2015
Impact Factor : 1.6200[UIF-2013]

Original Article

$ZnFe_2O_4$ nanocrystals: structural and magnetic properties

Nidhi Sharma, Sushil Kumar and Praveen Aghamkar

ABSTRACT

Nanophase zinc ferrite ($ZnFe_2O_4$) has been prepared by co-precipitation technique under stoichiometric conditions, followed by calcination at temperatures 673 and 1073 K. The effect of temperature on particle size has been studied using X-ray diffraction. The particle size of samples was in the range of 8.7-33.5nm. Fourier transform infrared spectroscopy confirmed the presence of zinc ferrite at all temperatures. The morphological studies were conducted by transmission electron microscopy, while the magnetic properties were demonstrated by vibrating sample magnetometer. The present study maintained that the physical quantities of zinc ferrite such as saturation magnetization, retentivity and coercive field, as acquired by VSM technique, are primarily dependent on the method of preparation and experimental conditions. The decrease in magnetization with increase in particle size may be due to super exchange interaction between Fe^{3+} ions on two sublattices A and B.

Keywords: Zinc ferrite; co-precipitation; XRD; FTIR; TEM; VSM.

Nidhi Sharma, Sushil Kumar and
Praveen Aghamkar

From
Material science lab, Chaudhary devi lal
university, Sirsa, Haryana, India.

The Article Is Published On March
2015 Issue & Available At
www.scienceparks.in

DOI:10.9780/23218045/1202013/49

Introduction

Currently magnetic nanoparticles are attracting significant interest due to their extensive applications, ranging from fundamental research to industrial use. Spinel ferrite nanocrystals are regarded as one of the most important inorganic nanomaterials because of their optical, electrical, magnetic and catalytic properties. Spinel ferrites are the materials of great potential because of their tremendous technological applications. The zinc ferrite series has been prepared at different temperature by co-precipitation technique[1,2]. Among the spinel ferrite systems, zinc ferrite ($ZnFe_2O_4$) is found to be most interesting to study its structural, morphological and magnetic properties [3]. The structure of spinel oxides AB_2O_4 consists of a closed packed FCC arrangement of oxygen atoms with two non-equivalent crystallographic sites A and B with tetrahedral and octahedral coordination. In case of $ZnFe_2O_4$, Zn^{2+} and Fe^{3+} distribution at A and B sites within the structure can be represented by the formula $[Zn_{\delta}Fe_{1-d}][Zn_{1-d}Fe_{1-d}]O_4$ where δ is the inversion parameter. For normal spinel system d = 1 and for inverse spinel system δ =0 [4,5]. For partly inverted spinel system   lies in between 0 and 1. The crystalline bulk form of $ZnFe_2O_4$ is a normal spinel with Zn_{2+} ions only on the A sites and Fe_{3+} ions only on the B sites and is characterized as an ordered anti-ferromagnet below 10 K [3]. In the present study, zinc ferrite nanocrystals were prepared from an aqueous solution containing metal nitrates and distilled water using a low temperature thermal treatment method, followed by grinding and then calcinations at higher temperature. This method, known as co-precipitation, is environmental friendly in the sense that it neither uses nor produces toxic substances, and it offers the advantage of simplicity, low cost and low reaction temperature [1,2]. The structural, micro-structural and magnetic properties of prepared zinc ferrite samples have been studied.

2. Experimental details

2.1 Preparation of samples

The zinc ferrite samples have been prepared by co-precipitation technique followed by heat treatment at different temperatures. The high purity reagents (Aldrich 99.99% purity): zinc nitrate $Zn(NO_3)_2.6H_2O$, ferric nitrate $Fe(NO_3)_3.2H_2O$, sodium hydroxide NaOH and distilled water were used to prepare the samples. $ZnFe_2O_4$ nanoparticles were prepared by adding 0.1 mol of zinc nitrate in 500 ml distilled water and 0.2 mol of ferric nitrate in 500 ml distilled water in a conical flask under constant stirring using a magnetic stirrer. During stirring the sodium hydroxide was added drop wise to maintain the pH of solution at about 10 at reaction temperature of 343K. The precipitate so formed was washed several times with distilled water and then filtered. The powder was dried in an oven at 373K. The as-prepared powdered samples of zinc ferrite were annealed at different temperatures 673,1073K for 4h which changes the crystallinity and hence the particle size.

2.2 Characterization of samples

Complementary methods were used to characterize the heat treated $ZnFe_2O_4$ samples. In order to determine the crystallite size and lattice constant, XRD patterns of samples were recorded by an X-ray diffractometer (Philips PW/1710) with Cu filter using monochromatic CuKa radiation of wavelength 1.548 Å at 50 KV and 40 mA, in the scanning range 2θ ~ 10-800. To investigate the particle size distribution and morphology of the samples, TEM micrograph was recorded using transmission electron microscope (Hitachi-H7500) at 100 KV. For this purpose, samples were dispersed in ethyl alcohol in an ultrasonic bath and then pipetted on a carbon-coated copper grid. To study the compositional characteristics from optical excitation of vibrational modes, infrared spectra were recorded in the range 4000-400 cm^{-1} using Fourier transform infrared spectrometer (Perkin Elmer 1600). For this purpose, pellets were obtained by homogeneously mixing the samples with KBr powder and then pressing. The saturation magnetization measurements were carried out by a search coil method. Polytronic power supply (model-BCS-1000), electromagnet (Type Hem-100) and flux meter (model-FM109) were used for this purpose.

3. Results and discussion

3.1 XRD studies

Fig. 2 illustrates the XRD patterns of as prepared sample (a) and samples thermally treated at different temperatures 673 K (b) and 1073 K (c) for 4 h. The diffraction pattern of as prepared sample shows broad peaks centered around 2θ~ 30.08, 35.42, 42.96, 53.26, 56.78, 62.320 and their respective Miller indices could be compared with standard XRD pattern of zinc ferrite. Chekcell program has been used to determine Miller indices (220), (311), (400), (422), (511), (440) of observed peaks in XRD patterns. The broad peaks suggest the poor crystallinity of as-prepared sample. The XRD pattern of sample (b) annealed at 673 K for 4 h exhibits sharp peaks. The increase in sharpness infers that the crystallinity of zinc ferrite increases on thermal treatment. It has space group Fd3m (cubic-0.8441nm, space group: Fd3m, Z=8; [ICDD PDF:22-1012] [6-8]. Here, it is worth mentioning that the traces of naturally occurred phases like Fe_2O_3 and ZnO in the pattern of zinc ferrite samples are absent. The absence of additional impurity phase formation, which is generally observed in ferrites synthesized by the conventional ceramic method [6-9], indicates that the co-precipitation results in the better quality samples having no impurity phases.

The crystallite size has been determined by the well known Debye-Scherrer formula [10]:

$$D = \frac{k\lambda}{\beta \cos\theta}$$

Where k is a constant (=0.9), D is the crystallite size in nm, β is the full width of the diffraction line at half of the maximum measured in radian, θ is the X-ray wavelength in nm and θ is the Bragg angle corresponding to a peak. The intensity of characteristic peaks not only increased but also their widths decreased significantly on increasing the annealing temperature because tiny crystallites fused together by melting their surfaces and as a result the crystallite size of zinc ferrite samples increased with temperature [11].The observed crystallite size is 8.7 and 33.5 nm of the samples annealed at 673 and 1073 K respectively.

The crystallite size of different samples has been determined and is given in Table 1. One may notice that the particle size almost increases linearly with increasing calcination temperature holds for 4h. It is expected that the enlargement of particle size is due to grain growth of sample as individual small particles merged together.

To determine the lattice strain present in the sample, Williamson-Hall equation is given by

$$\beta\cos\theta = \frac{k\lambda}{D} + 4\varepsilon \sin\theta$$

Where k= 0.9 for uniform small size crystals, θ is the wavelength of X- ray used, θ is the Bragg angle, is the strain and D is the average crystallite size. It is well known that the contributions of crystallite size and lattice strain to the broadening of peaks [12] are independent of each other. Due to the small crystallite size and lattice strain present in the material, the XRD peak broadening can be distinguished from W-H plot. We plot a graph between β cosθ and sinθ which comes out to be a straight line. The value of strain is estimated from the slope of the line and the crystallite size is estimated from the intercept on y-axis. The estimated crystallite size of material from this method is found to be in agreement with the Scherrer equation.

The X-ray density of a ferrite sample 'D_f' has been determined by the following relation [13]:

$$D_f = \frac{8M}{N a^3}$$

Where M is the sum of atomic weights of all the atoms in the unit cell (i.e. the molecular weight of zinc ferrite), N is the Avogadro's number and a^3 is the volume of cubic unit cell. Each unit cell of the spinel structure contains eight molecules. It has been observed that X-ray density of a sample increases with increase in annealing temperature and is shown in Table 1. It may be attributed to the decrease in lattice parameter of the sample on annealing.

3.2 FTIR studies

A pre-requisite for the interpretation of infrared spectra of zinc ferrite is the assignment of observed absorption bands in the spectra to particular vibrational mode within the structure of the ferrite. The assignment of infrared absorption bands are influenced by the oxidation state of the sample. The infrared spectra of as-prepared and annealed samples has been investigated to obtain the information of structure and the arrangement of building structural groups with respect to each other and the types of bonds present in the sample. The FTIR spectra of different samples were recorded in the wavenumber range of 400-4000 cm^{-1} of different samples. Spectrum (a) shows characteristic bands in different region of wavenumbers. In this spectrum, 551 and 441 cm-1 are typical characteristic bands of zinc ferrite [14], in which higher frequency bands attributes to intrinsic vibration of Zn-O (tetrahedral site) while lower frequency bands correspond to stretching vibration of Fe-O (octahedral site) [15,16]. This spectrum also shows H-O-H band overtones with the surface hydroxyl group vibration and results in the broadening of band around 1600 cm-1. The band around 1300 cm-1 is due to the banding modes of H-O-H absorbed at the surface. A very strong and broad band centered at 3387 cm^{-1} can be assigned to the peaks of H_2O. When the sample was heat treated at 673 K for 4 h, the FTIR traces clearly shows strengthening in zinc ferrite structure, while weakness in hydroxyl group. However, in case of sample thermally treated at 1073K for 4 h, the bands of hydroxyl groups are completely disappeared and the zinc ferrite valley shifts towards lower frequency.

From the force constant models for vibrational properties [17,18], the bond angle can be approximated by an expression of the form:

$$\nu = \nu_0 \sin(\frac{\theta}{2})$$

In our case,

θ_0 = 551 cm^{-1} for as prepared sample θ = 500, 543 cm^{-1} for samples heat treated at 673, 1073K respectively.

One may observe that with increase in annealing temperature, the high frequency bands shift towards lower wavenumber (red-shift). The frequency shift in FTIR spectra is related to the change of bonding characteristics such as bond angle and bond length. This IR analysis has been very useful for establishing the calcination temperature of 1073 K because it removed unwanted ions that may disturb the crystal lattice during preparation. The absorption bands observed within these specific frequency limits reveal the formation of single phase spinel structure.

3.3 TEM studies

TEM was employed to visualize the size and the shape of crystallites and to confirm the nano crystalline nature of the prepared samples. Fig. 6 shows the TEM images of zinc ferrite samples calcined at temperatures 673 and 1073 K. The micrographs of prepared samples reveal the compact arrangement of almost homogeneous nanoparticles with spherical shape. The particle size of a sample is increased with increasing calcination temperature. The images clearly show the agglomeration of nanoparticles which may be attributed to the magnetic dipole interactions between the particles. The smallest particle size obtained in this study was about 8.7 nm at 673 K and the largest size was about 33.57 nm at 1073 K. The particle size determined from TEM is in agreement with the particle size determined from XRD. This suggested that several neighboring particles fused together to increase the particle size due to the melting of their surfaces [19]. Moreover, a zoom on a representative particle confirms the high crystalline quality of a prepared material.

3.4 Magnetization studies

The room temperature magnetic properties of prepared $ZnFe_2O_4$ nanoparticles calcined at 673 and 1073K were investigated by the VSM technique in the range of -5000 to +5000 Gauss as shown in fig.8.The samples exhibited modified ferromagnetic magnetic behavior(shown in inset). The room temperature magnetic behavior of ferrite nanoparticles can be explained as the results of important factors such as cationic distribution in spinel structure, the heating rate of calcination, and the surface spin structure of nanoparticles. Although all these factors can be effective in magnetic behavior but their effects on the ferrite nanoparticles with different structures are not similar.

The values of retentivity (M_r), correcivity (H_c) and saturation magnetization (M_s) of the samples vary with calcination temperature and particle size and are given in Table 1. These data make it clear that the retentivity, correctivity and saturation magnetization decreases with increase in particle size. Cation inversion is one of the most important parameters that can be effective in the variation of the magnetic properties of zinc ferrite nanoparticles from that of their bulk counterpart. In bulk form, zinc ferrite has a normal spinel structure in which all the Zn^{2+} ions are in A-sites and Fe^{3+} ions are distributed in B-sites [20]. Moreover, in bulk form, zinc ferrite only occurs in intra-sublattice (B-B) exchange interactions and it does not have intra-sublattice (A-A) exchange interactions or inter-sublattice (A-B) super exchange interactions [21]. The inter-sublattice (A-B) super exchange interactions of the cations are much stronger than the (A-A) and the (B-B) interactions at nanoscale [22]. Due to cation inversion, which originates from heat treatment, the structure of $ZnFe_2O_4$ transfers from a normal spinel structure to a mixed spinel structure [21]. This cation inversion causes the zinc ferrite nanoparticles to experience inter-sublattice (A-B) super exchange interactions and intra-sublattice (A-A) exchange interactions in addition to intra-sublattice (B-B) exchange interactions. But, due to the degree of inversion, which is larger for smaller size particles, the saturation magnetization increases for smaller size particles [23], while it decreases with increase in calcination temperature. The decrease in lattice constant supports the decrease in degree of inversion, with increasing temperature as lattice constant varies directly with degree of inversion[24-28]. Also, decrease in magnetization may be attributed to the fact that with increase in temperature, domain rotation dominates over domain wall motion.

The particle size has been reported to influence the magnetic properties of materials. The saturation magnetization is decreased with increasing crystallite size of mono-domain particles due to the surface spin canting and thermal fluctuations [29]. The degree of inversion, the surface spin structure and the rate of calcination temperature increases the saturation magnetization in a sample having smaller size particles [30].

4. Conclusions

The present study explores the synthesis of pure nanocrystalline spinel zinc ferrite by a simple and cost-effective co-precipitation method. The structural and magnetic properties of zinc ferrites depend on experimental conditions. XRD patterns and TEM images show the formation of ZnFe2O4 nanoparticles having particle size in the range 8.7-33.5nm. FTIR confirmed the presence of zinc ferrite phase in the sample at all annealing temperatures. The change observed in the magnetic properties of $ZnFe_2O_4$ nanoparticles with particle size suggested that this could be a useful way to design and fabricate novel magnetic materials. Further, this method can be extended to the synthesis of other spinel ferrite nanoparticles of technological importance.

Acknowledgements

Authors are thankful to National Physical Laboratory, New Delhi, for providing experimental facilities.

References

[1] T.J. Shinde, A.B. Gadkari, P.N. Vasambekar, Mater. Chem. Phys., 111 (2008) 87.
[2] B.P. Rao. C.O. Kim, C.G. Kim, I. Dumitru, L. Spinu, O.F. Caltun, IEEE Trans. Magn., 42 (2006) 2858.
[3] C.N. Chinnasamy, A. Narayanasamy, N. Ponpandian, K. Chattopadhyay, H. Gureault, M.J. Greneche, J. Phys. Condens. Matter., 12 (2000) 7795.
[4] M.R. Anantharaman, S. Jagatheesan, K.A. Malini, S. Sindhu, J. Magn. Magn. Mater., 189 (1998) 83.
[5] G.F. Goya, H.R. Rechenberg, J. Appl. Phys., 87 (2000) 8005.
[6] P. Laokul, V Amornkitbamrung, S. Seraphin, Curr. Appl. Phys., 11 (2011) 101.
[7] L. Zhen, K. He, C.Y. Xu, J. Magn. Magn. Mater., 320 (2008) 2672.
[8] J. Jiang, Li. H, Mater. Lett., 64 (2010) 945.
[9] J.P. Singh, R.C. Srivastava, H.M. Agarwal, Nucl. Instrum. Methods Phys., 268 (2010) 1422.
[10] R. Jenkins, R.L. Snyder, Jhon Wiley & Sons Inc, New York, 1996.
[11] K.N. Yu, X. Yonghong, L. Yulong, X. Caoshui, Phys. Rev. B, 55 (1997) 2666.
[12] R. Yogamalar, R. Srinivasan, A. Vinu, K. Ariga, A.C. Bose, Solid State Commun., 149 (2009) 1919.
[13] T.J. Shinde, A.B. Gadkari, P.N. Vasambekar, J. Mater. Sci. Mater. Electron, 21 (2010) 120.
[14] P. Laokul, V. Amornkitbamrung, S. Seraphin, S. Maensiri, Curr. Appl. Phys., 11 (2011) 101.
[15] J.L. Martin, A. Lopez-Delgado, E. Vila, F.A. Lopez, J. Alloys Compds., 287 (1999) 276.
[16] A. Lopez, A. Lopez-Delgado, J.L. Martin de Vidales, E. Vila , J. Alloys Compds., 265 (1998) 291.
[17] P.N. Sen, M.F. Thorpe, Phys. Rev. B 15 (1977) 4030.
[18] G. Lucovsky, Philos. Mag. B 39 (1979) 513.
[19] Y. Qu, H. Yang, N. Yang, H. Zhu, G. Zou, Mater. Lett. 60 (2006) 3548.
[20] D.S. Mathew, R.S. Juang, Chem. Eng. J. 129 (2007) 51.
[21] F.S. Li, L. Wang, J.B. Wang, Q.G. Zhous, X.Z. Zhou, H.P. Kunkel. G. Williams, J. Magn. Magn. Mater., 268 (2004) 332.
[22] M. Atif, S.K. Hasanain, M. Nadeem, J. Sci. Commun 138 (2006) 416.
[23] M.K. Roy, B. Haldar, H.C. Verma, Nanotechnol., 17 (2006) 232.
[24] KRIESSMAN, C. J. and HARRISON, S. E., Phys. Rev. 103 (1956) 857.
[25] FALLER, J. G. and BIRCHENALL, C. E., J. Appl. Crystallogr. 3 (1970) 496.
[26] Mozzr, R. L. and PALEDINO, A. E.,J. Chem. Phys. 39 (1963) 435.
[27] VISHNEVSKII, L., ALAPIN, B., AKSEL'ROD, E. and SUKHA- REVSKII, B., IZV. A.N. SSSR, Neorgan. Mat 6 (1979) 1479.
[28] DE GRAVE, E., DE SITTER, J. and VANDENBERGHE, R., Appl. Phys. 7 (1975) 77.

[29] R.H. Kodama, A.E. Berkowitz, E.J. Mcniff, S. Foner, Phys. Rev. Lett., 77 (1996) 394.
[30] R.V. Upadhyay,Pramana 49(1997) 309.

Table 1: Structural and magnetic parameters of prepared zinc ferrite samples.

S.No.	Annealing temp. (^{0}C)	Particle size D (nm)	Lattice parameter a (Å)	X-ray density (g/cm^3)	Retentivity M_r (emu/g)	Coercivity H_c (gauss)	Saturation magnetization M_s (emu/g)
1	As prepared	8.7	8.4285	5.348	1.05	320	7.15
2	400	10.0	8.4247	5.355	0.35	380	2.16
3	800	33.5	8.4063	5.390	0.03	182	0.30

Figures caption

Fig. 1: Sintering programs of zinc ferrite
Fig. 2: XRD patterns of zinc ferrite samples calcined at different temperatures.
Fig. 3: Williamson-Hall plot of a zinc ferrite sample calcined at different temperatures .
Fig. 4: FTIR spectra of zinc ferrite samples calcined at different temperatures.
Fig. 5: Variation of frequency of characteristic absorption bands with calcinations temperatures.
Fig. 6: TEM images of zinc ferrite samples calcined at different temperatures.
Fig. 7: Histogram of TEM images
Fig. 8: M-H curves obtained at room temperature for zinc ferrite samples calcined at different temperatures.

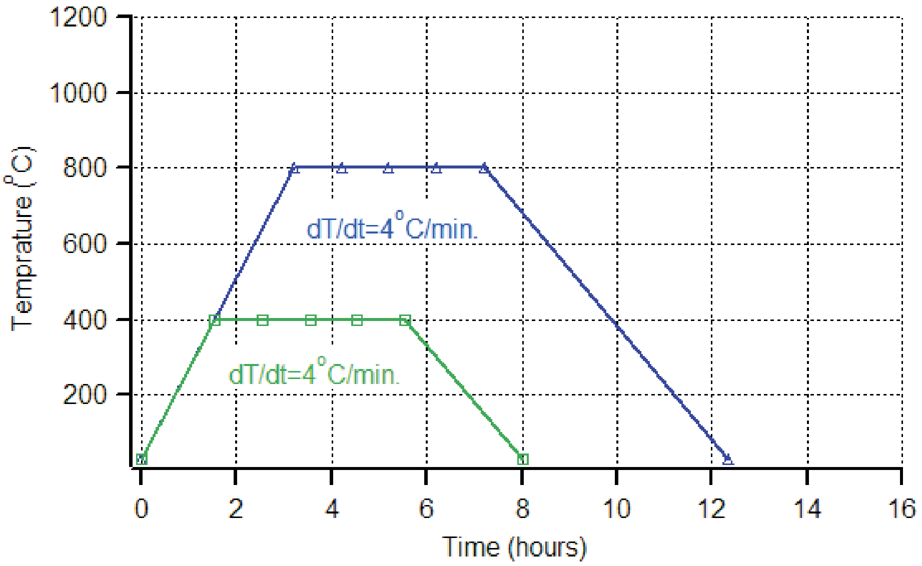

Fig. 1

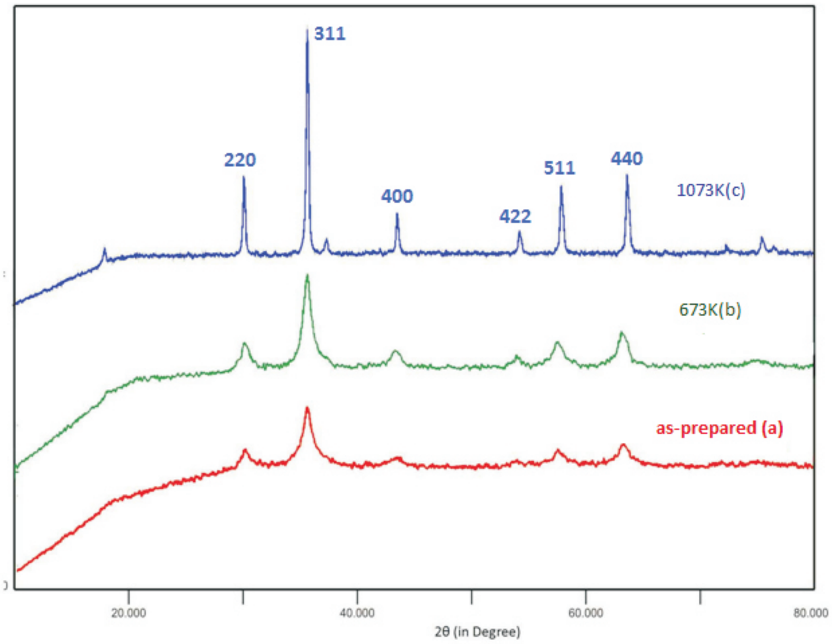
311
220
400
422
511
440
1073K(c)
673K(b)
as-prepared (a)
20.000
40.000
60.000
80.000
2θ (in Degree)

Fig.2

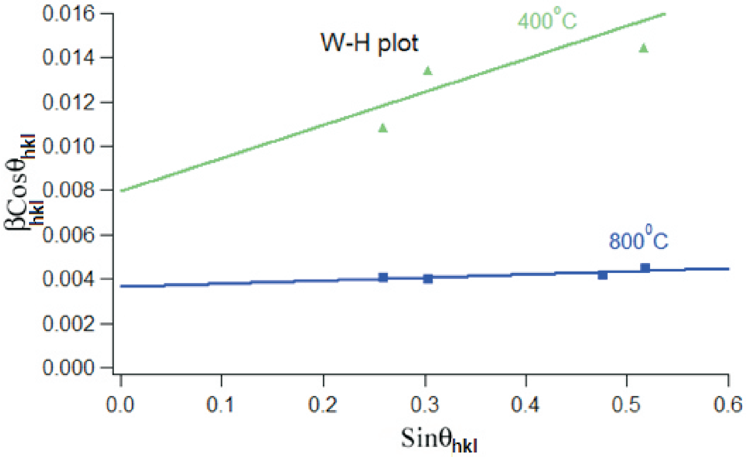
W-H plot
400°C
800°C
βCosθ_hkl
Sinθ_hkl
0.016
0.014
0.012
0.010
0.008
0.006
0.004
0.002
0.000
0.0
0.1
0.2
0.3
0.4
0.5
0.6

Fig.3

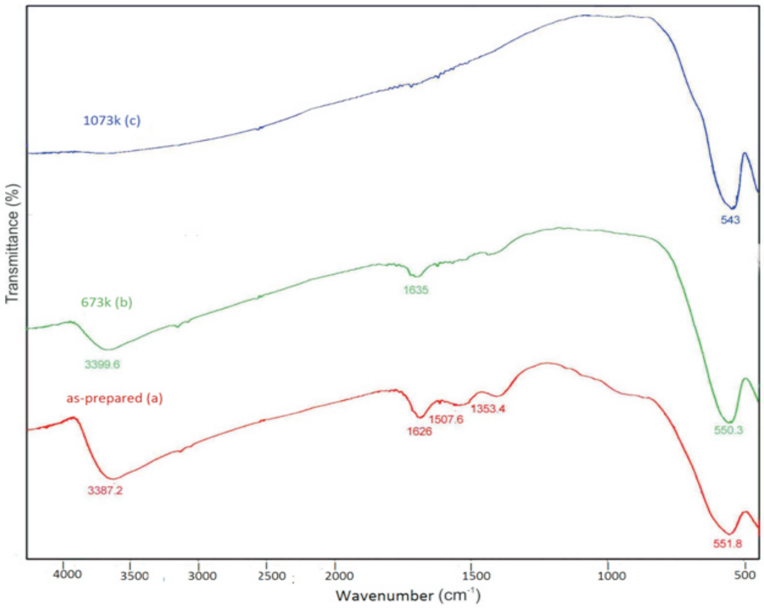
1073k (c)
543
673k (b)
1635
3399.6
550.3
as-prepared (a)
1626
1507.6
1353.4
3387.2
551.8
Transmittance (%)
4000
3500
3000
2500
2000
1500
1000
500
Wavenumber (cm⁻¹)

Fig.4

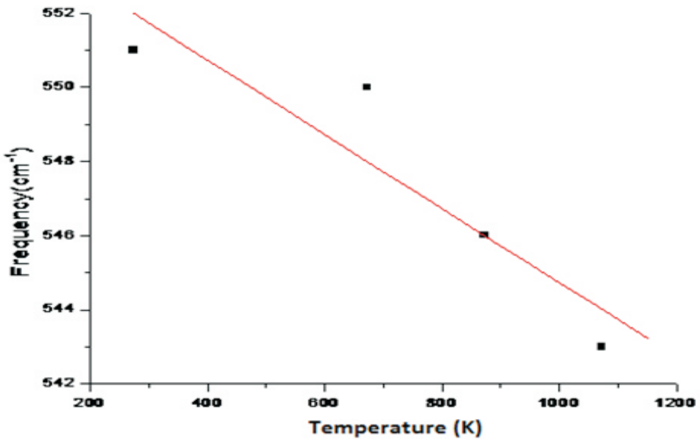
552
550
548
546
544
542
Frequency(cm⁻¹)
200
400
600
800
1000
1200
Temperature (K)

Fig.5

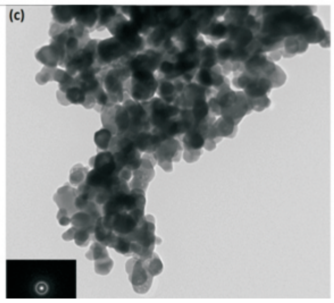
(c)

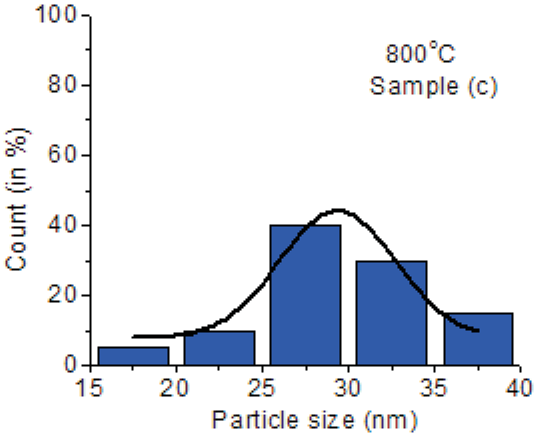
800°C
Sample (c)
Count (in %)
100
80
60
40
20
0
15
20
25
30
35
40
Particle size (nm)

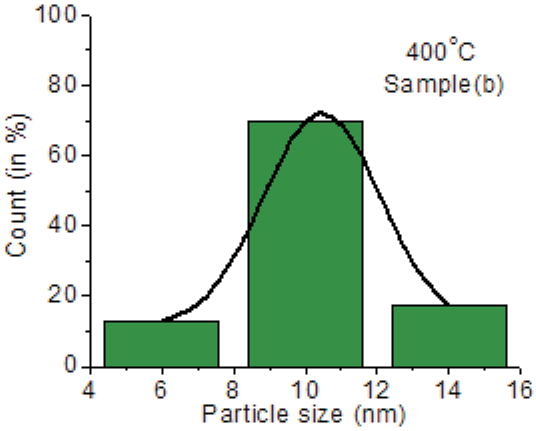
400°C
Sample(b)
Count (in %)
100
80
60
40
20
0
4
6
8
10
12
14
16
Particle size (nm)

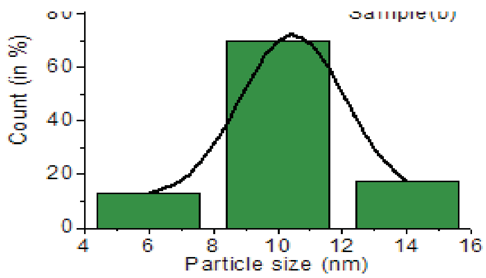
Count (in %)
60
40
20
0
4
6
8
10
12
14
16
Particle size (nm)

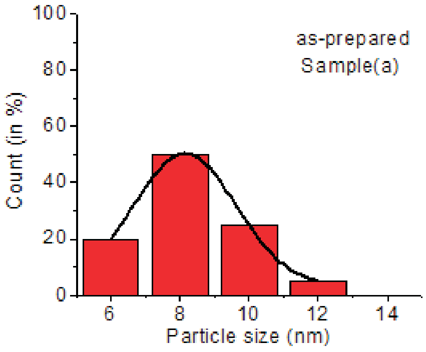
100
80
60
40
20
0
Count (in %)
6
8
10
12
14
Particle size (nm)
as-prepared
Sample(a)

Fig.7

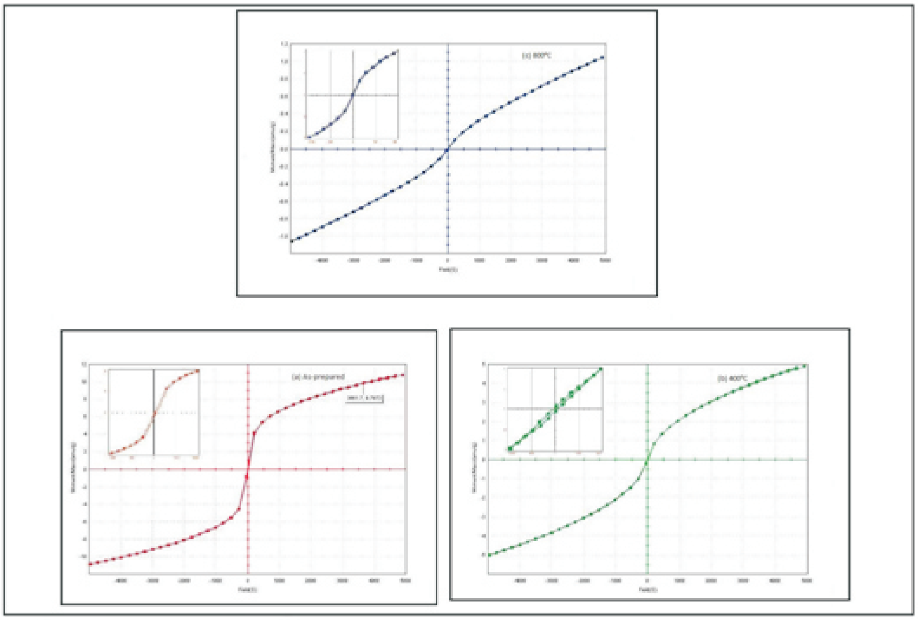
(c) 800°C
(a) As-prepared
(b) 400°C

Fig.8